

Persistence of weak ferromagnetism in antiferromagnetic systems on the body-centered octahedral lattice

E. Jurčišinová  and M. Jurčičin *Institute of Experimental Physics, Slovak Academy of Sciences, Watsonova 47, 040 01 Košice, Slovakia*

(Received 9 November 2023; accepted 23 January 2024; published 12 February 2024)

The possibility of existence of weak ferromagnetism in antiferromagnetic systems on the body-centered octahedral lattice is investigated in the framework of the corresponding spin-1/2 J_1 - J_2 model in the recursive-lattice approach. The exact solution of the model is found and its phase diagram is determined. The magnetic and thermodynamic properties of all phases are studied, the nature of all phase transitions is established, and an equation that determines the positions of all second-order phase transitions of the model is found. The magnetic and entropy properties of all ground states of the model are also determined. It is shown that the weak ferromagnetism predicted earlier in the pure spin-1/2 antiferromagnetic system on the octahedral lattice remains present even in the case of the model on the body-centered octahedral lattice with antiferromagnetic as well as ferromagnetic interactions between the central site of each elementary octahedron and each of its vertices. However, the presence of the interacting central site suppresses the weak ferromagnetism at very low temperatures, where the standard antiferromagnetic phase emerges. At the same time, the temperature region with the antiferromagnetic phase increases with simultaneous decreasing of the region, where the weak ferromagnetism can be observed, when the strength of the interaction between the central site of each elementary octahedron and each of its vertices increases. Moreover, the phenomenon of weak ferromagnetism disappears completely when this interaction becomes sufficiently stronger than the nearest-neighbor antiferromagnetic interaction between spin variables placed in vertices of each elementary octahedron of the lattice. Moreover, the possibility of the existence of the classical spin-liquid behavior in such magnetic systems is also discussed.

DOI: [10.1103/PhysRevE.109.024106](https://doi.org/10.1103/PhysRevE.109.024106)

I. INTRODUCTION

Geometrically frustrated antiferromagnetic systems [1–10], for which the impossibility of an unambiguous spin ordering in the zero-temperature limit is determined by the geometry of the lattice [11], exhibit many intriguing magnetic and thermodynamic properties. Among the most interesting properties of such magnetic systems are the formation of nontrivial discrete systems of ground states with high macroscopic degeneracy [12–14], the existence of the anomalous low-temperature behavior of the specific heat that leads to the appearance of significant magnetocaloric effects that can be used for the effective adiabatic (de)magnetization cooling to very low temperatures [15–28], and various theoretically described [5,9,29–47] and potentially experimentally observed [45,48–61] exotic quantum states such as states with spin-liquid behavior. Another interesting nontrivial phenomenon experimentally observed especially in various perovskite-type magnetic materials is the existence of the weak ferromagnetic behavior even in the antiferromagnetic systems [62–81].

From a theoretical point of view, it is quite clear that the full description of various frustrated magnetic systems can be achieved only by investigating relevant quantum models. However, as was pointed out, e.g., in Ref. [34], one of the main problems in the theoretical investigation of fundamental quantum properties of two-dimensional (and therefore also three-dimensional) spin systems is the nonexistence of even

nearly exact analytical or at least computational methods for analysis of such quantum systems on infinite lattices. In this situation, classical models can be helpful since it is well known that many basic properties of the frustrated magnetic systems can be understood even in the framework of the corresponding simplified classical models (such as the Ising and Ising-like models), which can be studied in a much more precise way, and therefore the obtained results can have fundamental relevance. Moreover, it is also well known that even exact solutions of some classical frustrated systems can be found in the case of the two-dimensional models, although only in the zero external magnetic field [12,13].

In this respect, recent theoretical investigations of the corresponding classical models [82,83] have shown that the presence of the aforementioned weak ferromagnetism seems to be a quite natural behavior of the antiferromagnetic systems with octahedral structure, which is the basic geometric structure of the perovskites. More specifically, it was shown in Ref. [82] in the framework of the exactly solvable spin-1/2 antiferromagnetic Ising model on the octahedral recursive lattice that the simultaneous presence of geometric frustration and bipartite properties of the antiferromagnetic model on the octahedral lattice can naturally lead to the appearance of weak ferromagnetic behavior with small but nonzero total magnetization below the critical (Néel) temperature. The possibility of the existence of such a nontrivial behavior was subsequently confirmed within a completely different theoretical approach,

namely, using the six-site cluster effective field theory approximation [83].

At the same time, due to the simplicity of the model studied in Refs. [82,83], in the sense that the model contains only pure nearest-neighbor antiferromagnetic interaction and the geometry of the octahedral lattice, it seems that the theoretical studies [82,83] describe the simplest possible mechanism for the very existence of weak ferromagnetism in the frustrated antiferromagnetic systems. As was already mentioned, weak ferromagnetism is generated through the simultaneous presence of the geometric frustration (given by the presence of eight triangles in each elementary octahedron of the octahedral lattice) and the bipartite properties of the model (given by presence of three four-site cycles in each elementary octahedron of the octahedral lattice).

However, it is also clear that, on the one hand, the ideal lattice magnetic systems do not exist and, on the other hand, very often, various additional interactions can be present in the studied systems that can significantly change their total magnetic properties. In this respect, a quite natural question immediately arises, namely, whether weak ferromagnetism in the antiferromagnetic system on the octahedral lattice will exist (or preserve its existence) in such magnetic systems when various additional interactions are present since, without a doubt, their presence can significantly change the aforementioned geometric properties of the pure antiferromagnetic model on the octahedral lattice, which are responsible for the very existence of the phenomenon of the weak ferromagnetism.

In this respect, in this paper we intend to investigate in detail the influence of the presence of the interacting spin variables in the centers of all elementary octahedra on the magnetic and thermodynamic properties of the pure antiferromagnetic system on the octahedral lattice. Our main goal is to determine whether the weak ferromagnetism, which seems to be a natural aspect of pure antiferromagnetic systems on the octahedral lattice, can preserve its existence even under the influence of additional antiferromagnetic or ferromagnetic interactions between spin variables placed in the centers of all elementary octahedra and spin variables placed in their vertices. This problem will be studied using the recursive-lattice approximation, i.e., we will analyze the corresponding classical spin-1/2 J_1 - J_2 Ising model on the recursive body-centered octahedral lattice that takes into account basic geometric properties of the regular three-dimensional body-centered octahedral lattice responsible for frustration. It is worth mentioning that the recursive approximation used represents an extension of the well-known Bethe lattice approximation [84]. The main advantage of such an approach is the fact that the exact solution of the model can be found and, as a result, all magnetic and thermodynamic properties of the model can be studied in the exact way. As will be shown, the presence of such additional interaction in the antiferromagnetic system on the octahedral lattice not only preserves the possibility of the existence of the weak ferromagnetic behavior but, under some conditions, can also lead to the appearance of the classical spin-liquid behavior in such magnetic systems.

The paper is organized as follows. In Sec. II the model is defined and its exact solution is presented. In Sec. III the phase

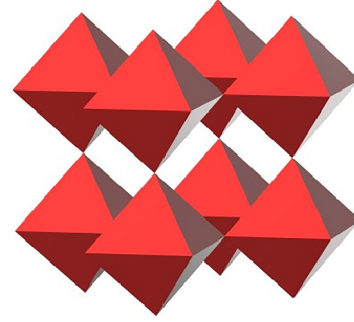


FIG. 1. Basic structure of the regular octahedral lattice.

diagram of the model is found, its magnetization properties are discussed, and all phase transitions are identified. The thermodynamics of the model is discussed in Sec. IV. In Sec. V the main results of the paper are reviewed and discussed.

II. FORMULATION OF THE MODEL AND ITS EXACT SOLUTION

As was already mentioned in Introduction, our aim is to investigate in detail the influence of the presence of the central spin in each elementary octahedron on the magnetic as well as thermodynamic properties of the antiferromagnetic system on the octahedral lattice (see Fig. 1) in the framework of the corresponding classical spin-1/2 J_1 - J_2 model on the octahedral recursive lattice (see Fig. 2), where each elementary octahedron has the internal structure explicitly shown in Fig. 3. In what follows, the regular three-dimensional octahedron lattice with the elementary structure shown in Fig. 3 will be referred to as the body-centered octahedral (BCO) lattice. Similarly, the recursive octahedron lattice with this elementary structure will be referred to as the recursive BCO lattice.

As follows from Fig. 3, the model exhibits two different interactions between adjacent sites, namely, the interaction J_1 between all nearest-neighbor pairs of spin variables in the vertices of each elementary octahedron, which is always antiferromagnetic ($J_1 < 0$), and the interaction J_2 between the spin variable placed in the center of each elementary octahedron (denoted by D in Fig. 3) and each individual spin variable placed in the corresponding vertex of the same octahedron. In addition, we will suppose that this interaction can have

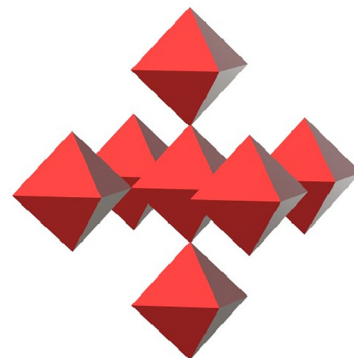


FIG. 2. Basic structure of the octahedral recursive lattice.

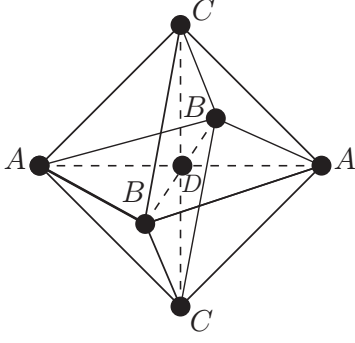


FIG. 3. Structure of each elementary octahedron of the BCO lattice and of the recursive BCO lattice. The symmetry of the model requires one to consider the existence of four different sublattices denoted by A , B , C , and D . All solid lines represent the antiferromagnetic interaction J_1 and all dashed lines represent pair interactions J_2 between the central site (sublattice D) and sites in all vertices of the elementary octahedron (sublattices A , B , and C), which can be antiferromagnetic as well as ferromagnetic.

antiferromagnetic ($J_2 < 0$) as well as ferromagnetic ($J_2 > 0$) character.

Thus, the Hamiltonian of the model has the form

$$\mathcal{H} = -J_1 \sum_{\langle ij \rangle} s_i s_j - J_2 \sum_{\langle ik \rangle} s_i s_k, \quad (1)$$

$$Z = \sum_{s_n^{(A_1)}, s_n^{(B_1)}, s_n^{(C_1)}, s_n^{(D)}} \exp \left\{ K_1 \left[(s_n^{(A_1)} + s_n^{(A_2)})(s_n^{(B_1)} + s_n^{(B_2)} + s_n^{(C_1)} + s_n^{(C_2)}) + (s_n^{(B_1)} + s_n^{(B_2)})(s_n^{(C_1)} + s_n^{(C_2)}) \right] \right\} \\ \times \exp \left[K_2 s_n^{(D)} (s_n^{(A_1)} + s_n^{(A_2)} + s_n^{(B_1)} + s_n^{(B_2)} + s_n^{(C_1)} + s_n^{(C_2)}) \right] u_n(s_n^{(A_1)}) u_n(s_n^{(A_2)}) v_n(s_n^{(B_1)}) v_n(s_n^{(B_2)}) w_n(s_n^{(C_1)}) w_n(s_n^{(C_2)}). \quad (3)$$

Here it is supposed that the recursive BCO tree has n layers, $s_n^{(X_i)}$ for $X \in \{A, B, C\}$ and $i \in \{1, 2\}$ represent the spin variables of two different sites on the sublattice X within the central octahedron, $s_n^{(D)}$ represents the corresponding spin variable of the central site of the central octahedron, and $u_n(s_n^{(A_i)})$, $v_n(s_n^{(B_i)})$, and $w_n(s_n^{(C_i)})$ represent the partition functions of six independent branches of the whole recursive BCO tree with base sites A_i , B_i , and C_i , respectively, through which they are connected to the central octahedron. The quantities $u_n(s_n^{(A_i)})$, $v_n(s_n^{(B_i)})$, and $w_n(s_n^{(C_i)})$ for $i = 1$ and 2 can be determined recursively by solving the corresponding system of recursive relations. However, it is more suitable to work with a simpler system of three independent recursion relations for

where each spin variable s_i acquires one of the two possible values ± 1 and J_1 and J_2 are the aforementioned two interactions of the model. Therefore, the first sum in Eq. (1) runs over all nearest-neighbor lattice sites placed in the vertices of elementary octahedrons of the BCO lattice (the solid lines in Fig. 3) and the second sum runs over all nearest-neighbor pairs of the spin variables, one of which is placed in the center of an elementary octahedron of the lattice and the second is placed in one of its six vertices (the dashed lines in Fig. 3). Note that the analysis of the geometrically frustrated model studied dictates the necessity to consider the existence of four independent sublattices denoted by A , B , C , and D (see Fig. 3).

Since we intend to analyze the model described by the Hamiltonian (1) on the corresponding recursive lattice that approximates the regular BCO lattice (see Fig. 2), the general partition function of the model

$$Z \equiv \sum_s e^{-\beta \mathcal{H}} = \sum_s \exp \left(K_1 \sum_{\langle ij \rangle} s_i s_j + K_2 \sum_{\langle ik \rangle} s_i s_k \right), \quad (2)$$

where $\beta = 1/k_B T$, T is the temperature, k_B is the Boltzmann constant, $K_1 = \beta J_1$, $K_2 = \beta J_2$, and the sum over s is taken over all possible spin configurations on the lattice, can be rewritten in the recursive form (see Ref. [84] for the general technical details of the recursive-lattice technique)

quantities x_n , y_n , and z_n defined by the ratios

$$x_n = u_n(+)/u_n(-), \quad (4)$$

$$y_n = v_n(+)/v_n(-), \quad (5)$$

$$z_n = w_n(+)/w_n(-). \quad (6)$$

For instance, the recursion relation for x_n has the explicit form

$$x_n = \frac{X_1(x_{n-1}, y_{n-1}, z_{n-1})}{X_0(x_{n-1}, y_{n-1}, z_{n-1})}, \quad (7)$$

where

$$X_1(a, b, c) = a \{ 2b [c^2 e^{4K_1} \cosh(4K_2) + 2c \cosh(2K_2) + e^{-4K_1}] + b^2 [c^2 e^{12K_1} \cosh(6K_2) + 2c e^{4K_1} \cosh(4K_2) + e^{-4K_1} \cosh(2K_2)] + (c^2 + 1) e^{-4K_1} \cosh(2K_2) + 2c e^{-4K_1} \} + b^2 [c^2 e^{4K_1} \cosh(4K_2) + 2c \cosh(2K_2) + e^{-4K_1}] + 2b [(c^2 + 1) \cosh(2K_2) + 2c] + c^2 e^{-4K_1} + e^{4K_1} \cosh(4K_2) + 2c \cosh(2K_2) \quad (8)$$

and

$$X_0(a, b, c) = a \{ b^2 [c^2 e^{4K_1} \cosh(4K_2) + 2c \cosh(2K_2) + e^{-4K_1}] + 2b [(c^2 + 1) \cosh(2K_2) + 2c] + c^2 e^{-4K_1} + 2c \cosh(2K_2) + e^{4K_1} \cosh(4K_2) \} + b^2 [(c^2 + 1) e^{-4K_1} \cosh(2K_2) + 2c e^{-4K_1}] + e^{12K_1} \cosh(6K_2) + 2b [c^2 e^{-4K_1} + 2c \cosh(2K_2) + e^{4K_1} \cosh(4K_2)] + c^2 e^{-4K_1} \cosh(2K_2) + 2c e^{4K_1} \cosh(4K_2). \quad (9)$$

At the same time, due to the symmetry of the studied model, the recursion relations for y_n and z_n in Eqs. (5) and (6) are also defined by functions X_1 and X_0 with the appropriate interchange of the variables, namely,

$$y_n = \frac{X_1(y_{n-1}, x_{n-1}, z_{n-1})}{X_0(y_{n-1}, x_{n-1}, z_{n-1})}, \quad (10)$$

$$z_n = \frac{X_1(z_{n-1}, y_{n-1}, x_{n-1})}{X_0(z_{n-1}, y_{n-1}, x_{n-1})}. \quad (11)$$

The physical properties of all possible phases of the studied model are driven by the physically relevant (real and positive)

stable fixed points of the system of three recursion relations (7), (10), and (11) with coordinates x , y , and z obtained in the limit $n \rightarrow \infty$, i.e., $x = \lim_{n \rightarrow \infty} x_n$, $y = \lim_{n \rightarrow \infty} y_n$, and $z = \lim_{n \rightarrow \infty} z_n$.

For completeness, let us also note that the coordinates x , y , and z of each stable fixed point of the recursion relations (7), (10), and (11) must belong to the set of all solutions of the system of three polynomial equations with respect to x , y , and z obtained from the recursion relations (7), (10), and (11) in the limit $n \rightarrow \infty$. For instance, the corresponding polynomial equation obtained from the recursion relation (4) can be written as

$$\begin{aligned} & -e^{8K_1} \cosh(4K_2) \{x^2(y^2z^2 + 1) - 2x[y^2z + y(z^2 - 1) - z] - y^2z^2 - 1\} - \cosh(2K_2)(yz + 1) \\ & \times [2e^{4K_1}(x^2 - 1)(y + z) + x(yz - 1)] + e^{16K_1}x \cosh(6K_2)(y^2z^2 - 1) - 4e^{4K_1}(x^2 - 1)yz - x^2(y^2 + z^2) \\ & - 2x(y^2z + yz^2 - y - z) + y^2 + z^2 = 0. \end{aligned} \quad (12)$$

At the same time, due to the symmetry of the studied problem, the equations that correspond to the recursion relations (10) and (11) can be again obtained directly from Eq. (12) by a simple interchange of variables $x \leftrightarrow y$ and $x \leftrightarrow z$, respectively.

When (for given values of the parameters of the model) a single physically relevant stable fixed point of the recursion relations (7), (10), and (11) exists it describes the magnetic as well as thermodynamic properties of the corresponding unique phase of the model. However, more than one such recursively stable fixed point can exist for given values of the model parameters that correspond to possible different phases of the model. In such situations, the knowledge of the free energy can be used to determine which phase represents the genuine thermodynamically stable phase of the model. In this respect, the thermodynamically stable phase is the phase described by the recursively stable fixed point, for which the value of the free energy is the smallest. In our case, the free energy per site f of the studied model can be derived using, e.g., the technique described in Ref. [85] and has the form

$$\beta f = \frac{1}{4} \ln \left(\frac{e^{4K_1+6K_2} F_1^2}{F_2 F_3 F_4} \right), \quad (13)$$

where

$$\begin{aligned} F_1 = & e^{16K_1}(e^{12K_2} + 1)(x^2y^2z^2 + 1) + 2(e^{8K_2} + 1)e^{8K_1+2K_2}[x^2yz(y+z) + xy^2z^2 + x + y + z] \\ & + 4[x^2yz + x(y^2z + yz^2 + y + z) + yz](e^{4K_2} + 1)e^{4(K_1+K_2)} + 16xyz e^{4K_1+6K_2} + 4e^{6K_2}[x^2(y+z) \\ & + x(y^2 + z^2) + yz(y+z)] + e^{4K_2}(e^{4K_2} + 1)[x^2(y^2 + z^2 + 1) + y^2(z^2 + 1) + z^2], \end{aligned} \quad (14)$$

$$\begin{aligned} F_2 = & (e^{8K_2} + 1)e^{8K_1+2K_2}(x^2y^2z + 2x + 2y + z) + 2(e^{4K_2} + 1)e^{4(K_1+K_2)}[x^2yz + x(y^2z + 2y + z) + yz] + 8xyz e^{4K_1+6K_2} \\ & + e^{16K_1}(e^{12K_2} + 1) + 2e^{6K_2}(x^2(2y + z) + 2xy^2 + y^2z) + e^{4K_2}(e^{4K_2} + 1)[x^2(y^2 + 1) + y^2], \end{aligned} \quad (15)$$

and the explicit form of the functions F_3 and F_4 can be obtained from the function F_2 by the interchange of the variables $z \leftrightarrow x$ and $z \leftrightarrow y$, respectively.

Finally, let us note that the existence of the explicit expression for the free energy per site of the model as a function of the model parameters and of the coordinates of the fixed points of the system of the recursion relations makes the model exactly solvable, i.e., it allows one to perform not only a complete analysis of the phase transitions but also to investigate in detail its thermodynamics.

III. PHASE DIAGRAM AND MAGNETIZATION PROPERTIES OF THE MODEL

Let us start with the investigation of the magnetization properties of the model, which will also allow us to identify all model phases. Since four different sublattices denoted by

A , B , C , and D must be considered for an unambiguous description of the model (see Fig. 3), four different sublattice magnetizations per site m_A , m_B , m_C , and m_D have to be defined ($m_X \equiv \langle s_n^{(X)} \rangle$, $X = A, B, C$, or D) with the total magnetization per site $m = (m_A + m_B + m_C + m_D)/4$, which has the explicit form

$$m = \frac{m_1}{2m_0}, \quad (16)$$

where

$$\begin{aligned} m_1 = & e^{16K_1}(2e^{12K_2} + 1)(x^2y^2z^2 - 1) + (3e^{8K_2} + 1) \\ & \times e^{8K_1+2K_2}[x^2yz(y+z) + x(y^2z^2 - 1) - y - z] \\ & + 4e^{4K_1+8K_2}\{x^2yz + x[y^2z + y(z^2 - 1) - z] - yz\} \\ & + e^{8K_2}(x^2(y^2 + z^2 - 1) + y^2(z^2 - 1) - z^2) \end{aligned} \quad (17)$$

and

$$\begin{aligned}
 m_0 = & e^{16K_1}(e^{12K_2} + 1)(x^2y^2z^2 + 1) + 2(2e^{8K_2} + 1) \\
 & \times e^{8K_1+2K_2}[x^2yz(y+z) + xy^2z^2 + x + y + z] \\
 & + 4[x^2yz + x(y^2z + yz^2 + y + z) + yz](e^{4K_2} + 1) \\
 & \times e^{4(K_1+K_2)} + 16xyz e^{4K_1+6K_2} + 4e^{6K_2}[x^2(y+z) \\
 & + x(y^2 + z^2) + yz(y+z)] + e^{4K_2}(e^{4K_2} + 1) \\
 & \times [x^2(y^2 + z^2 + 1) + y^2(z^2 + 1) + z^2], \quad (18)
 \end{aligned}$$

where, as always, x , y , and z are coordinates of the corresponding physically relevant stable fixed point of the system of the recursion relations given in Eqs. (7), (10), and (11).

As was already mentioned, our aim is to investigate the influence of the presence of the central spin variables in each elementary octahedron of the BCO lattice on its properties in the framework of the studied recursive-lattice approximation. For this purpose, it is convenient to define the parameter $\alpha = J_2/|J_1|$ as well as the reduced temperature $k_B T/|J_1|$ and to investigate various model properties as functions of these two independent dimensionless parameters. In this case, the assumption $\alpha = 0$ leads to the pure antiferromagnetic model on the recursive octahedral lattice studied in Ref. [82] but with noninteracting spin-1/2 atoms present in the centers of all elementary octahedra of the lattice. Note, however, that the presence of such noninteracting particles in the model changes the numerical values of some quantities such as the total magnetization per site, but qualitatively the model is completely equivalent to the model without the presence of such a ‘‘decoration’’ studied in Ref. [82].

The analysis performed in Ref. [82] in the framework of the antiferromagnetic model on the recursive octahedral lattice without the spin variables present in the centers of the elementary octahedra has predicted the existence of the weak ferromagnetic behavior below the critical temperature with a very small but nonzero total magnetization. It is worth mentioning that the possibility of the existence of weak ferromagnetism in the antiferromagnetic system on the octahedral lattice was also confirmed in the framework of the corresponding effective field theory analysis [83].

In this respect, as follows from Figs. 4 and 5, where the dependence of the absolute value of the total magnetization of the model on the reduced temperature $k_B T/|J_1|$ is shown for various relatively small negative and positive values of the parameter α ($0 \leq |\alpha| \leq 1$), i.e., for small antiferromagnetic as well as ferromagnetic values of the interaction J_2 , the presence of the weak ferromagnetic behavior remains preserved even when the interaction J_2 is switched on but is restricted to a temperature interval, the length of which decreases with the increasing of the absolute value of α . At the same time, these temperature intervals are the same for the antiferromagnetic and ferromagnetic cases. However, the absolute value of the total magnetization exhibits different behavior for the ferromagnetic ($J_2 > 0$) case in comparison to the antiferromagnetic ($J_2 < 0$) case. For convenience, let us denote these two phases with weak ferromagnetism present by WF₁ (for $\alpha < 0$) and WF₂ (for $\alpha > 0$).

The analysis also shows that the presence of the antiferromagnetic form of the weak ferromagnetism (i.e., for $J_2 < 0$)

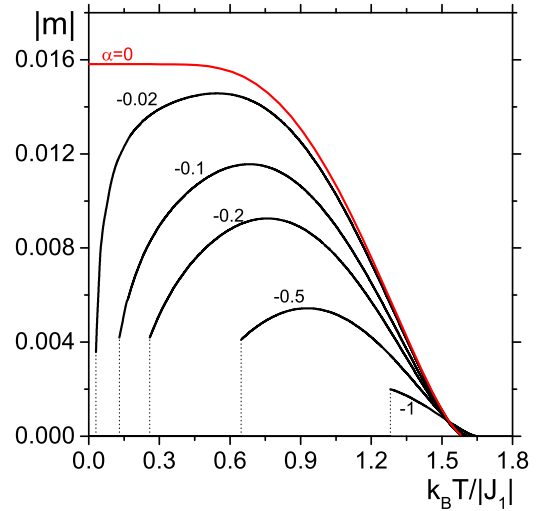


FIG. 4. Absolute value of the total magnetization of the model as a function of the reduced temperature $k_B T/|J_1|$ for various negative values of the parameter α from the interval $-1 \leq \alpha \leq 0$, i.e., when the interaction J_2 has antiferromagnetic character.

as well as of the ferromagnetic form (i.e., for $J_2 > 0$) completely disappears when $|\alpha| > 1.31$. Moreover, for any given value of the parameter α from the interval $0 < |\alpha| < 1.31$, there exists an interval of low temperatures for which another phase is realized with zero value of the total magnetization. At the same time, as it also follows from Figs. 4 and 5, the transition between this phase and the phase WF₁ or WF₂ (for a given value of the parameter α from the interval $0 < |\alpha| < 1.31$) is realized at the corresponding transition temperature of the first-order phase transition, at which the phase with zero total magnetization and the phase WF₁ or

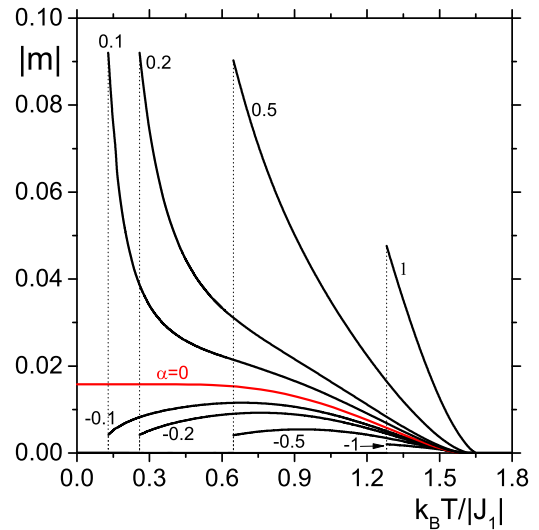


FIG. 5. Temperature dependence of the absolute value of the total magnetization of the model for various positive values of the parameter α from the interval $0 \leq \alpha \leq 1$, i.e., when the interaction J_2 is ferromagnetic. The corresponding total magnetization curves for negative values of α are also shown for comparison (see also Fig. 4).

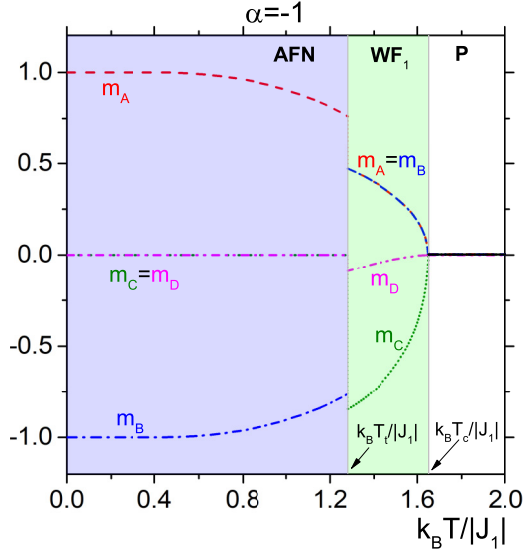


FIG. 6. Dependence of the sublattice magnetizations m_A , m_B , m_C , and m_D on the reduced temperature $k_B T/|J_1|$ for $\alpha = -1$ with the first-order phase transitions between the antiferromagnetic phase AFN (see the text) and weak ferromagnetic phase WF_1 at the corresponding transition temperature $k_B T_i/|J_1|$ as well as with the second-order phase transitions between the weak ferromagnetic phase WF_1 and the paramagnetic phase P at the corresponding critical temperature $k_B T_c/|J_1|$.

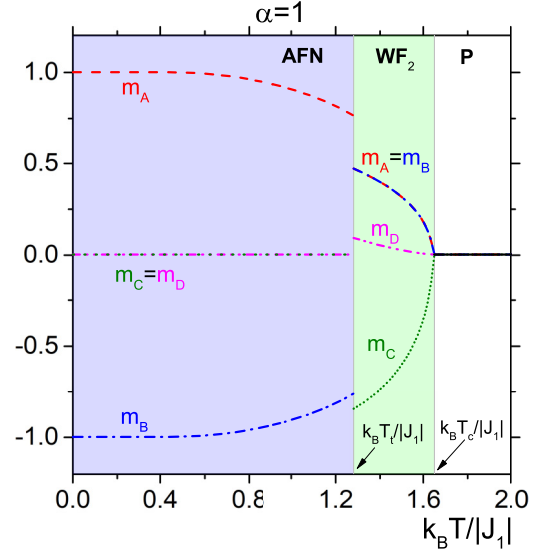


FIG. 7. Dependence of the sublattice magnetizations m_A , m_B , m_C , and m_D on the reduced temperature $k_B T/|J_1|$ for $\alpha = 1$ with the first-order phase transitions between the antiferromagnetic phase AFN (see the text) and weak ferromagnetic phase WF_2 at the corresponding transition temperature $k_B T_i/|J_1|$ as well as with the second-order phase transitions between the weak ferromagnetic phase WF_2 and the paramagnetic phase P at the corresponding critical temperature $k_B T_c/|J_1|$.

WF_2 coexist. To understand the essence of this phase, it is necessary to analyze the behavior of all sublattice magnetizations of the model as functions of the reduced temperature. In this respect, the typical behavior of all sublattice magnetizations of the model in the interval $0 < |\alpha| < 1.31$ is shown explicitly in Figs. 6 and 7 for $\alpha = -1$ and $\alpha = 1$, respectively, in the case with positive total magnetization of phases WF_1 and WF_2 (see Figs. 4 and 5). Note that, due to the symmetry among sublattices A, B, and C, there also exist physically equivalent solutions with mutual exchange of the sublattice magnetizations m_A , m_B , and m_C .

As follows from Figs. 6 and 7, the phase realized at low temperatures with the zero total magnetization behaves as a genuine antiferromagnetic (Néel) phase with two nonzero sublattice magnetizations that have the same absolute value but different signs (the sublattice magnetizations m_A and m_B in Figs. 6 and 7) and with zero value of the sublattice magnetization m_D as well as of one of the other sublattice magnetizations (the sublattice magnetization m_C in Figs. 6 and 7). It is also worth mentioning that this antiferromagnetic phase has completely the same magnetization properties as in the case with $-1.31 < \alpha < 0$ as well as for $0 < \alpha < 1.31$ and, in what follows, will be referred to as the AFN phase.

It is interesting that, as also follows from Figs. 6 and 7, the difference between weak ferromagnetic phases WF_1 and WF_2 is given only by a different behavior of the sublattice magnetization m_D , i.e., of the magnetization on the central sites of the elementary octahedra. More specifically, in the case of a positive value of the total magnetization m , the m_D is negative for the phase WF_1 and is positive for the phase WF_2 . Note that the absolute value of m_D is the same in both cases.

At the same time, the sublattice magnetizations m_A , m_B , and m_C behave completely identically, namely, two of them are equal to each other ($m_A = m_B$ in Figs. 6 and 7) and the third one has a different value as well as sign.

The realization of the first-order phase transitions between phase AFN and phases WF_1 and WF_2 at the corresponding reduced transition temperature $k_B T_i/|J_1|$ is also clearly visible on the sublattice magnetization level in Figs. 6 and 7. On the other hand, the transitions from phases WF_1 and WF_2 to the paramagnetic phase (denoted by P in Figs. 6 and 7) are the second-order phase transitions realized at the corresponding critical temperature $k_B T_c/|J_1|$.

For completeness, let us also note that for $\alpha = 0$ the weak ferromagnetic phase exists down to zero temperature, where the corresponding ground state is formed with the absolute value of the total magnetization $|m| \approx 0.01581$. This magnetization value is equal to $3/4$ of the absolute value of the total magnetization $|m| = 0.02108$ obtained in Ref. [82] within the antiferromagnetic spin-1/2 Ising model on the pure octahedral recursive lattice (without the presence of central sites within each elementary octahedron). The difference is caused by different numbers of spin variables in these two cases, with respect to which the total magnetization is calculated.

As was already mentioned, the weak ferromagnetic phases WF_1 and WF_2 are realized in the interval $0 < |\alpha| < 1.31$. On the other hand, the analysis shows that the antiferromagnetic phase AFN exists up to $|\alpha| < 4$ with the same magnetization properties and with direct transition from the phase AFN to the paramagnetic phase P at the corresponding critical temperatures of the second-order phase transitions in the interval

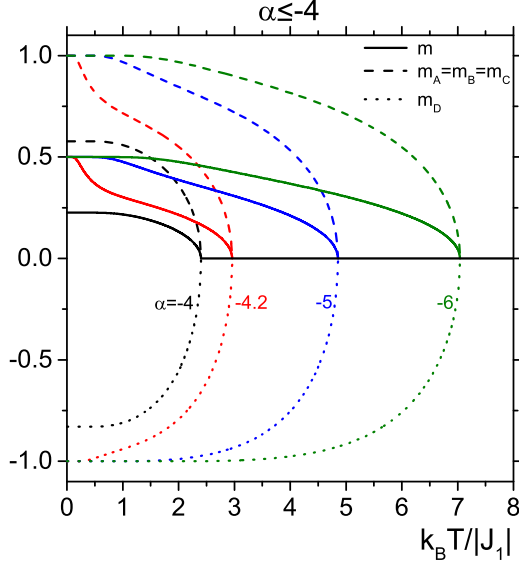


FIG. 8. Behavior of the total magnetization m and of the sublattice magnetizations m_A , m_B , m_C , and m_D of the model (in the case with positive values of the total magnetization) as a function of the reduced temperature $k_B T / |J_1|$ for various values of the parameter $\alpha \leq -4$ with the explicit formation of two different ground states for $\alpha = -4$ and $\alpha < -4$.

$1.31 < |\alpha| < 4$. Also note that, for a given absolute value of α from the interval $1.31 < |\alpha| < 4$, the value of the corresponding reduced critical temperature is again the same for $\alpha < 0$ and $\alpha > 0$.

Finally, the behavior of the total magnetization m of the model in the case of its positive value together with the corresponding behavior of the sublattice magnetizations m_A , m_B , m_C , and m_D as a function of the temperature is shown for various values $|\alpha| \geq 4$ in Figs. 8 and 9. The analysis shows (as it is also clear from Figs. 8 and 9) that, for a given absolute value of the parameter $|\alpha| \geq 4$, the sublattice magnetizations m_A , m_B , and m_C are always equal to each other. Moreover, their values do not depend on the sign of the parameter α . At the same time, the absolute value of the sublattice magnetization m_D is also independent of the sign of α , but m_D is negative when $\alpha < 0$ and is positive when $\alpha > 0$ (in the case when total magnetization is positive). Note also that the absolute value of m_D is equal to the value of $m_A = m_B = m_C$ at zero temperature but only for $\alpha > 4$. In this case, $m_A = m_B = m_C = |m_D| = 1$ at zero temperature.

It is also evident in Fig. 9 that the phase formed for $\alpha \geq 4$ has clear ferromagnetic properties with the saturated magnetization $|m| = 1$ in the zero-temperature limit for $\alpha > 4$ and with the second-order phase transitions to the paramagnetic phase at the corresponding reduced critical temperature. Therefore, for convenience, let us denote this phase by F. However, it is also evident that two different ground states are formed from this phase in the zero-temperature limit. One of them is a single-point-like ground state formed for $\alpha = 4$ with the absolute value of the total magnetization

$$|m| = \frac{23\sqrt{3} - \sqrt{2}}{60} \approx 0.64038 \quad (19)$$

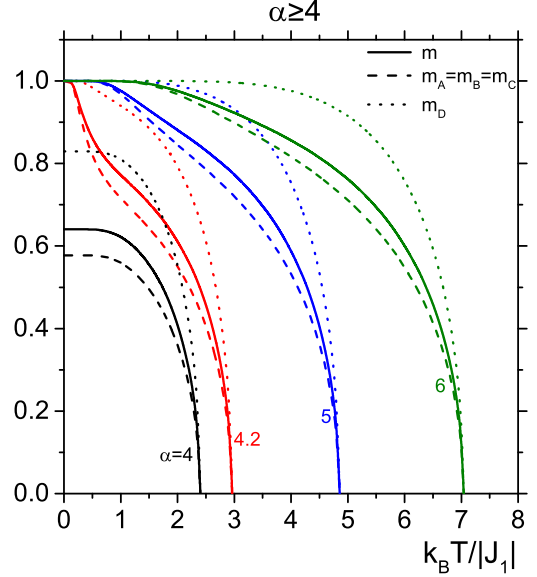


FIG. 9. Behavior of the total magnetization m and of the sublattice magnetizations m_A , m_B , m_C , and m_D of the model (in the case with positive values of the total magnetization) as a function of the reduced temperature $k_B T / |J_1|$ for various values of the parameter $\alpha \geq 4$ with the explicit formation of two different ground states for $\alpha = 4$ and $\alpha > 4$.

and the second one is the aforementioned saturated plateaulike ground state with the absolute value of the total magnetization $|m| = 1$ realized for $\alpha > 4$ in the zero-temperature limit.

On the other hand, the phase formed for $\alpha \leq -4$ also exhibits a nonzero value of total magnetization (see Fig. 8). However, since in this case all interactions are antiferromagnetic within the spin-1/2 model, for convenience, let us denote this phase by AF. At the same time, it is again easy to see that this phase also splits into two different ground states in the zero-temperature limit. One of them is another single-point-like ground state formed for $\alpha = -4$ with the absolute value of the total magnetization

$$|m| = \frac{7\sqrt{3} + \sqrt{2}}{60} \approx 0.22564 \quad (20)$$

and the second one is the plateaulike ground state with $|m| = 0.5$.

Thus, all phases of the model are identified now with first-order phase transitions between the antiferromagnetic phase AFN and the weak ferromagnetic phases WF₁ and WF₂. On the other hand, all phase transitions into the paramagnetic phase P are second-order phase transitions at the corresponding critical points. All of them are determined by the same general equation, the explicit form of which can be written as

$$\begin{aligned} & (-4e^{4(K_1+K_2)} + e^{2(4K_1+K_2)} - 4e^{4(K_1+2K_2)} \\ & + e^{4(4K_1+3K_2)} - 4e^{4K_1+6K_2} + e^{8K_1+10K_2} \\ & + e^{16K_1} - e^{4K_2} - 6e^{6K_2} - e^{8K_2})(8e^{4(K_1+K_2)} \\ & + 4e^{2(4K_1+K_2)} + 8e^{4(K_1+2K_2)} + e^{4(4K_1+3K_2)} \\ & + 8e^{4K_1+6K_2} + 4e^{8K_1+10K_2} + e^{16K_1} - e^{4K_2} - e^{8K_2}) = 0, \end{aligned} \quad (21)$$

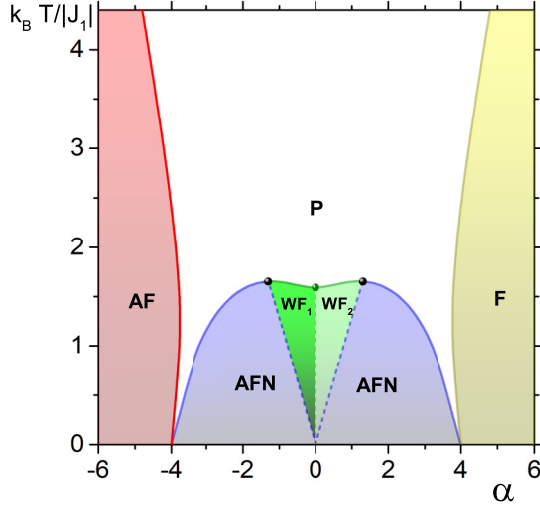


FIG. 10. Phase diagram of the model in the plane α versus $k_B T/|J_1|$ with six different phases (see the text). All solid curves represent the second-order phase transitions between any ordered phase and the paramagnetic one (P). The dashed curves between the genuine antiferromagnetic phase AFN and two phases WF_1 and WF_2 with weak ferromagnetism present denote the first-order phase transitions, which end on the corresponding curves of the second-order phase transitions at the critical points with coordinates $\{\alpha, k_B T_c/|J_1|\} \approx \{\pm 1.31, 1.6522\}$ (see the two black circles). The dashed line for $\alpha = 0$ that ends at the critical point $k_B T_c/|J_1| \approx 1.59259$ represents the weak ferromagnetic phase of the model without the interaction J_2 .

and, after simple algebraic manipulations, one can find that the critical temperature $k_B T_c/|J_1|$ for a given value of the parameter α is given as

$$\frac{k_B T_c}{|J_1|} = \frac{2}{\ln q_c}, \quad (22)$$

where q_c is the unique real solution of the equation

$$\begin{aligned} & (q^{6\alpha} - 4q^{3(\alpha+2)} - q^{4(\alpha+2)} - 4q^{2(\alpha+3)} + q^{\alpha+4} - q^{2(\alpha+4)} \\ & - 4q^{2(2\alpha+3)} - 6q^{3\alpha+8} + q^{5\alpha+4} + 1)(q^{6\alpha} + 8q^{3(\alpha+2)} \\ & - q^{4(\alpha+2)} + 8q^{2(\alpha+3)} + 4q^{\alpha+4} - q^{2(\alpha+4)} + 8q^{2(2\alpha+3)} \\ & + 4q^{5\alpha+4} + 1) = 0 \end{aligned} \quad (23)$$

with respect to q with the natural condition $q > 1$. Note that both factors in Eq. (23) are important since they determine the second-order phase transitions from different phases into the paramagnetic one.

The full phase diagram of the model in the plane α versus $k_B T/|J_1|$ is shown in Fig. 10, where all solid curves represent positions of the second-order phase transitions from all ordered phases into the paramagnetic phase P. At the same time, the first-order phase transitions between the phase AFN and any of two phases with the weak ferromagnetic behavior present (phases WF_1 and WF_2) are denoted by the two corresponding dashed curves. Note that these curves end on the curves of the second-order phase transitions at the critical points with coordinates $\{\alpha, k_B T_c/|J_1|\} \approx \{\pm 1.31, 1.6522\}$ (see the two corresponding black circles in Fig. 10). Finally,

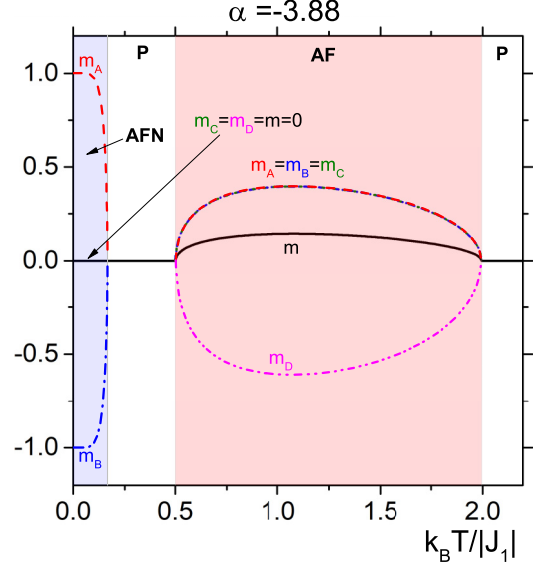


FIG. 11. Behavior of the total magnetization m and of the sublattice magnetizations m_A, m_B, m_C , and m_D of the model (in the case with positive values of the total magnetization) as a function of the reduced temperature $k_B T/|J_1|$ for $\alpha = -3.88$ with the existence of three consecutive second-order phase transitions.

the central dashed line, i.e., the dashed line for $\alpha = 0$ that separates phases WF_1 and WF_2 , which ends at the critical point $\{\alpha, k_B T_c/|J_1|\} \approx \{0, 1.59259\}$ (see the central circle in Fig. 10), represents the weak ferromagnetic phase in the model without the interaction J_2 , which corresponds to the weak ferromagnetic phase studied in Ref. [82].

The form of the curves of the second-order phase transitions between the antiferromagnetic phase AF and the paramagnetic phase as well as between the ferromagnetic phase F and the paramagnetic one (see Fig. 10) shows that there exist a small interval of the parameter α , namely, $3.78 < |\alpha| < 4$, for which the phase AF exists even for $\alpha > -4$ and the phase F exists even for $\alpha < 4$. The existence of this reentrant phenomenon in the studied model can also be seen in the behavior of the magnetization. In this respect, the temperature dependence of the total and sublattice magnetizations of the model (in the case with the total magnetization $m \geq 0$) is shown in Figs. 11 and 12 for $\alpha = -3.88$ and $\alpha = 3.88$, respectively, where three consecutive second-order phase transitions are present, namely, the phase transition from the phase AFN to the paramagnetic phase P followed by the phase transition from the paramagnetic phase to the antiferromagnetic phase AF (for $\alpha = -3.88$) or ferromagnetic phase F (for $\alpha = 3.88$) and, finally, from the phase AF or from the phase F back to the paramagnetic phase. Note that the existence of the reentrant behavior is a relatively widespread type of magnetic behavior especially in spin glasses (see, e.g., Refs. [86–89] and references cited therein).

It is also instructive to discuss briefly the typical dependence of the total magnetization and all sublattice magnetizations as a function of the parameter α for a given value of the reduced temperature. In this respect, such a dependence is shown in Figs. 13 and 14 for $k_B T/|J_1| = 1$ in the case with a positive value of total magnetization m .

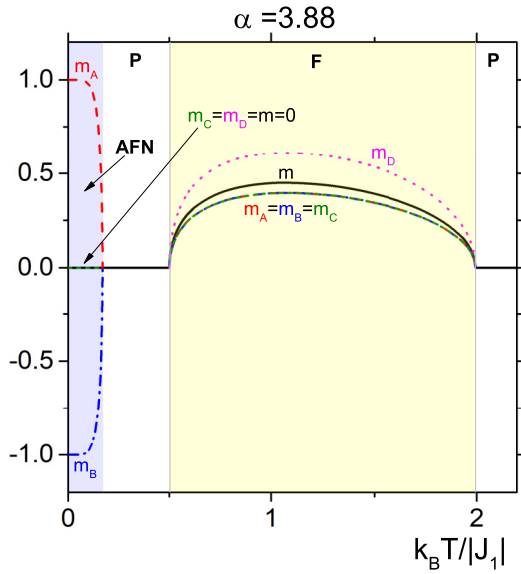


FIG. 12. Behavior of the total magnetization m and of the sublattice magnetizations m_A , m_B , m_C , and m_D of the model (in the case with positive values of the total magnetization) as a function of the reduced temperature $k_B T / |J_1|$ for $\alpha = 3.88$ with the existence of three consecutive second-order phase transitions.

As follows from Fig. 13, from the pure total magnetization behavior of the model, one can unambiguously identify the positions of two second-order and two first-order phase transitions. At the same time, as follows from Fig. 14, where the behavior of all sublattice magnetizations is present, the model exhibits two additional second-order phase transitions, which are invisible in the total magnetization behavior. Finally, the magnetization properties of all ground states of the model are shown in Fig. 15, where the existence of three different

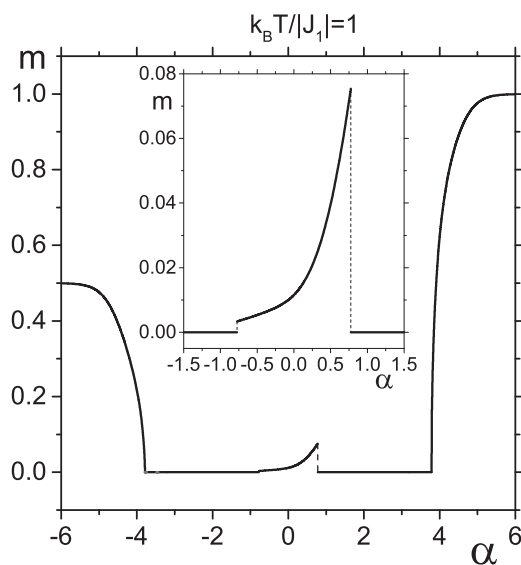


FIG. 13. Behavior of the total magnetization m of the model as a function of the parameter α for the reduced temperature $k_B T / |J_1| = 1$ with the evident presence of two second-order and two first-order phase transitions.

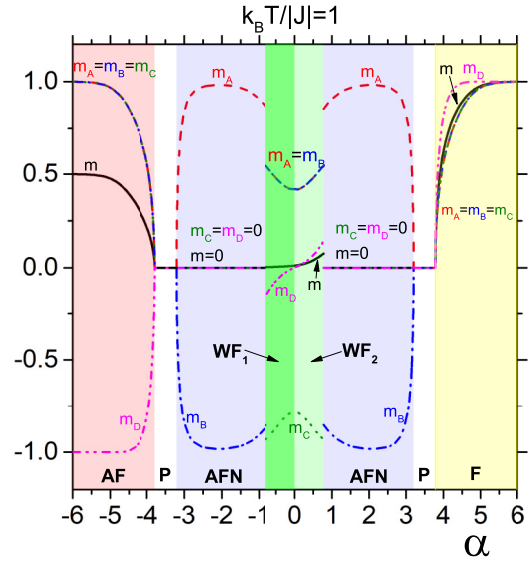


FIG. 14. Same behavior of the total magnetization m as in Fig. 13 together with the corresponding behavior of all sublattice magnetizations m_A , m_B , m_C , and m_D with the clear presence of four second-order and two first-order phase transitions between various phases of the model.

plateaulike ground states and three different single-point-like ground states can be clearly seen.

For completeness, let us also note that, since, in terms of critical phenomena, the studied model on the BCO lattice (like any model on an arbitrary recursive lattice) belongs to the mean-field class of universality, all critical exponents of the model are equal to those of the mean-field theory.

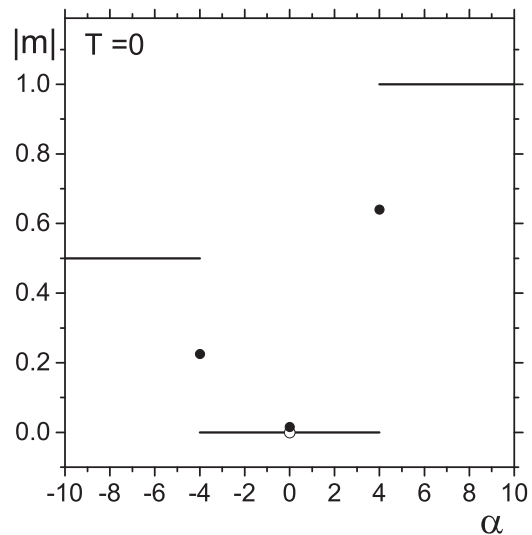


FIG. 15. Magnetization properties of all ground states of the model. The plateaulike ground states are formed for the AF phase with $|m| = 0.5$ (formed for $\alpha < -4$), for the AFN phase with $m = 0$ (formed in the interval $0 < |\alpha| < 4$), and for the F phase with saturated magnetization $|m| = 1$ (formed for $\alpha > 4$), which are separated by three different single-point-like ground states formed at $\alpha = -4$ with $|m| \approx 0.22564$, at $\alpha = 0$ with $|m| \approx 0.01581$, and at $\alpha = 4$ with $|m| \approx 0.64038$.

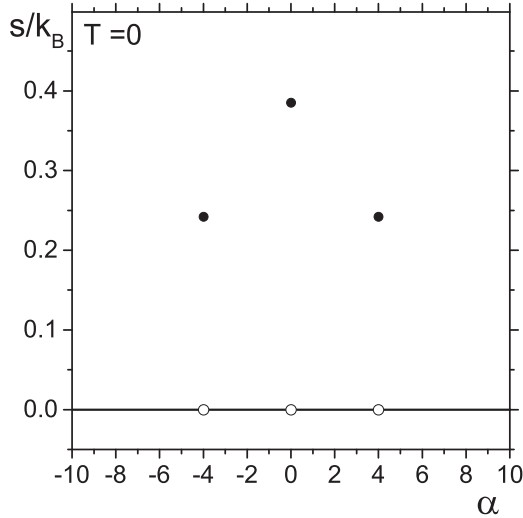


FIG. 16. Entropy properties of all ground states of the model. The entropy of all plateaulike ground states is equal to zero. On the other hand, all single-point-like ground states are highly macroscopically degenerated with the same values of the residual entropy $s \approx 0.24203 k_B$ as the ground states formed at $\alpha = \pm 4$ and $s \approx 0.38533 k_B$ as the most degenerated ground state of the model formed at $\alpha = 0$.

IV. ENTROPY AND SPECIFIC HEAT OF THE MODEL

Having the explicit expression for the free energy per site of the model given in Eqs. (13)–(15) as a function of the model parameters and of the coordinates of the fixed points of the recursive relations (7), (10), and (11), one not only can investigate the phase transitions of the model but also study its thermodynamic properties. In this respect, in what follows, we will be interested in its entropy properties through the analysis of the entropy per site $s \equiv -\partial f/\partial T$ of the model as well as in its specific-heat properties through the analysis of the specific heat at the constant magnetic field $c_H \equiv T\partial s/\partial T = -T\partial^2 f/\partial T^2$.

First, it is important to stress that the thermodynamic properties of the model depend on the absolute value of the parameter α but are independent of its sign. This nontrivial property of the studied model is seen, e.g., in Fig. 16, where the entropy properties of all model ground states are shown. As follows from this figure, all plateaulike ground states of the model have zero entropy. On the other hand, all three single-point-like ground states realized for $\alpha = 0$ and ± 4 are highly macroscopically degenerated with the residual entropy per site

$$s = \frac{k_B}{4} \ln \left(1 + 2\sqrt{\frac{2}{3}} \right) \approx 0.24203 k_B \quad (24)$$

valid for $\alpha = \pm 4$ and

$$s \approx 0.38533 k_B \quad (25)$$

obtained for $\alpha = 0$. Note that this value is different from the corresponding residual entropy per site $s \approx 0.28272 k_B$ of the antiferromagnetic model on the recursive octahedral lattice without the central spin variables [90] since, in the case of the presence of the noninteracting ($\alpha = 0$)

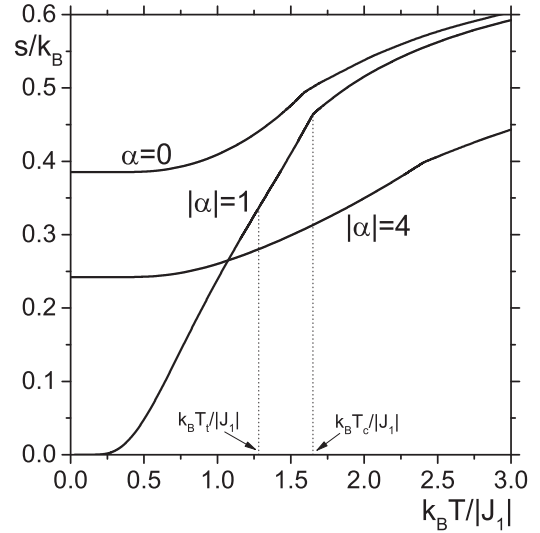


FIG. 17. Dependence of the entropy of the model on the reduced temperature for $|\alpha| = 0$ and 4 with the explicit formation of nonzero residual entropies as well as for $|\alpha| = 1$, which represents typical entropy behavior of the model in the interval $0 < |\alpha| < 1.31$ with the first- and second-order phase transitions present at the corresponding transition ($k_B T_t/|J_1|$) and critical ($k_B T_c/|J_1|$) temperatures, respectively.

central sites with spin $1/2$, they contribute to the total entropy per site of the system by the maximal entropy $k_B \ln 2$. This fact increases the total value of the residual entropy per site of the studied system to the value given in Eq. (25).

The formation of these two residual entropies is explicitly shown in Fig. 17, where the temperature dependence of the entropy per site of the model is shown for $|\alpha| = 0$ and 4 as well as for $|\alpha| = 1$, which represents the typical entropy behavior of the model in the interval $0 < |\alpha| < 1.31$, where two consecutive phase transitions are present. The first of them is the first-order phase transition from the phase AFN into the phase WF₁ or WF₂ at the corresponding transition temperature $k_B T_t/|J_1|$ with very small discontinuity in the entropy behavior and the second one is the second-order phase transition from the phase WF₁ or WF₂ into the paramagnetic phase P (see Fig. 10) at the corresponding critical temperature $k_B T_c/|J_1|$. The presence of these two consecutive phase transitions is more clearly visible in the behavior of the specific heat shown in Fig. 18.

The existence of the highly macroscopically degenerated ground states formed at $|\alpha| = 0$ and 4 should naturally lead to the formation of the anomalous second (Schottky) peak in the temperature dependence of the specific heat at low temperatures in their vicinity related to the presence of large entropy changes. Such behavior is demonstrated in Figs. 19 and 20, where the temperature dependence of the entropy (Fig. 19) and of the specific heat (Fig. 20) is shown for $|\alpha| = 4.2$ with the explicit presence of the Schottky peak in the specific-heat behavior at low temperatures as well as with discontinuity at the reduced critical temperature of the second-order phase transition from the phase AF (for $\alpha = -4.2$) or F (for $\alpha = 4.2$) into the paramagnetic one. Of course, similar behavior is also expected for α from the left vicinity of $|\alpha| = 4$. However,

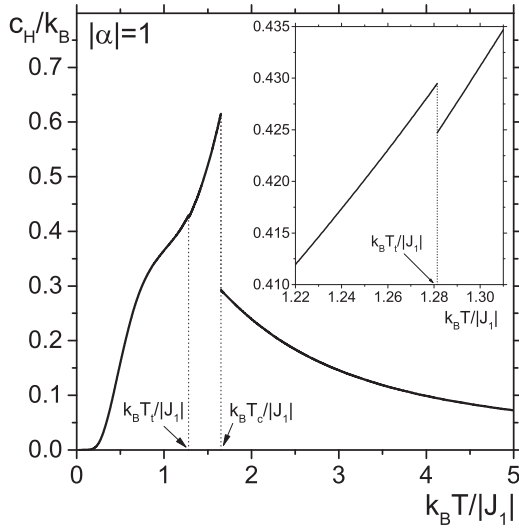


FIG. 18. Temperature dependence of the specific heat of the model for $|\alpha| = 1$, which represents typical behavior of the specific heat in the interval $0 < |\alpha| < 1.31$ with two discontinuities present at the transition and critical temperatures.

as can be seen in Figs. 21 and 22, where the temperature dependence of the entropy and specific heat of the model is shown for $|\alpha| = 3.88$, the anomalous low-temperature behavior of the specific heat is completely suppressed by the large changes of the specific heat related to the presence of the second-order phase transition from the phase AFN into the paramagnetic phase at the critical temperature denoted by $k_B T_{c_1} / |J_1|$.

For completeness, it is also instructive to present a typical dependence of the entropy per site as well as of the specific

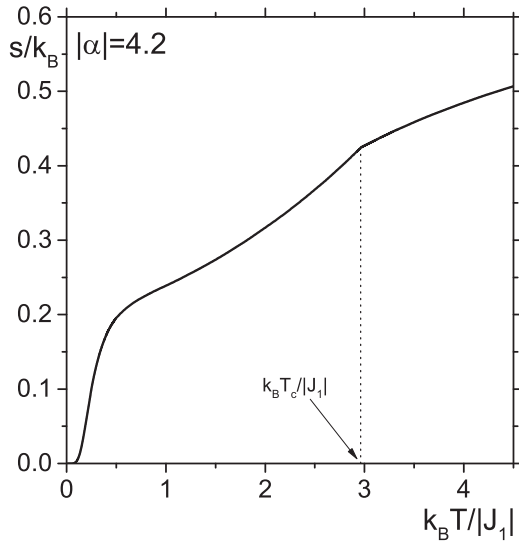


FIG. 19. Temperature dependence of the entropy per site of the model for $|\alpha| = 4.2$, which leads to the appearance of the anomalous (Schottky) behavior of the specific heat (see Fig. 20). The critical temperature $k_B T_c / |J_1|$ denotes the position of the second-order phase transition from the AF or F phase to the paramagnetic one (see Fig. 10).

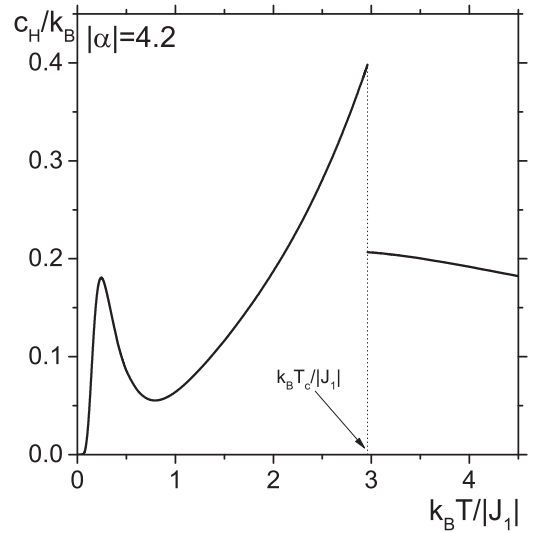


FIG. 20. Temperature dependence of the specific heat of the model for $|\alpha| = 4.2$ with the explicit presence of the additional (Schottky) peak at low temperatures.

heat of the model on the parameter α at low enough temperatures. Such a dependence is shown in Figs. 23 and 24 for $k_B T / |J_1| = 1$, where the presence of all six phase transitions between various phases is demonstrated. The explicit formation of giant entropy spikes at low temperatures in the vicinity of $\alpha = 0$ and $|\alpha| = 4$ is also visible here, which is related to the existence of two different highly macroscopically degenerated single-point-like ground states formed for $\alpha = 0$ and $|\alpha| = 4$ in the zero-temperature limit (see Fig. 16). Note that such behavior of the entropy is typical for frustrated magnetic systems (see, e.g., Refs. [22,91]).

Finally, let us also briefly discuss the following interesting fact that allows one to think about the possibility of the existence of spin-liquid-like behavior within the studied model.

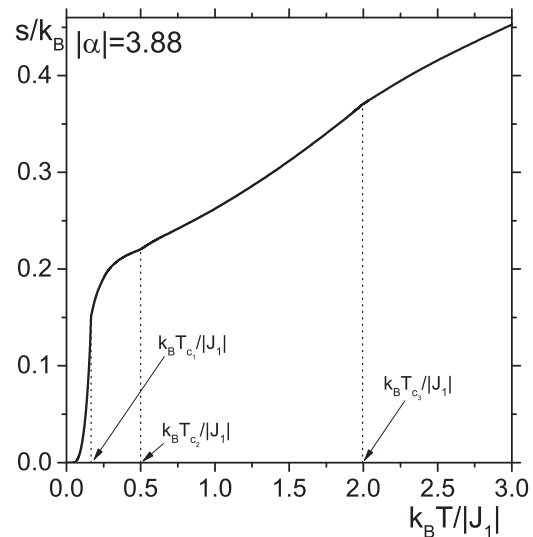


FIG. 21. Temperature dependence of the entropy per site of the model for $|\alpha| = 3.88$ with three consecutive second-order phase transitions.

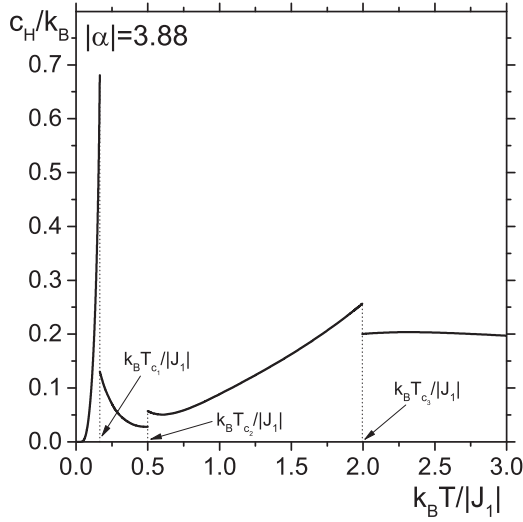


FIG. 22. Temperature dependence of the specific heat of the model for $|\alpha| = 3.88$ with three consecutive second-order phase transitions.

As follows from the phase diagram of the model shown explicitly in Fig. 10, the paramagnetic phase exists even down to zero temperatures in the close vicinity of the frustrated highly macroscopically degenerated ground states formed at $\alpha = \pm 4$. The closeness to these highly macroscopically degenerated ground states means that the paramagnetic phase in these regions is also highly degenerated. Moreover, as also follows from Fig. 10, the paramagnetic phase in these regions is bounded from the left and from the right by the curves of the second-order phase transitions. This means that the paramagnetic phase in these regions is (i) highly

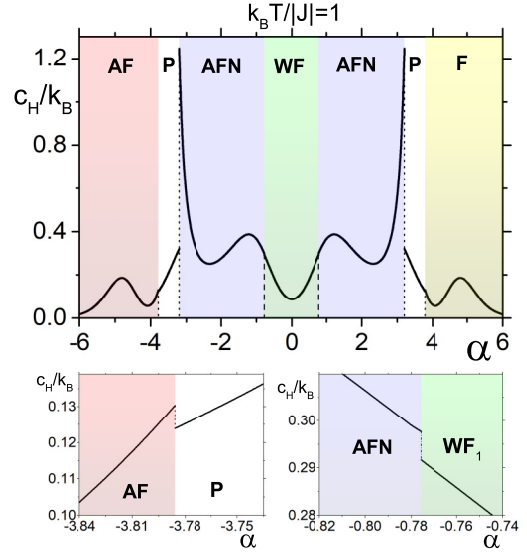


FIG. 24. Dependence of the specific heat of the model on the parameter α for $k_B T/|J_1| = 1$ with two first-order (dashed vertical lines) and four second-order (dotted vertical lines) phase transitions explicitly present between corresponding phases.

degenerated, (ii) highly correlated, and (iii) without the presence of strong thermal fluctuations, i.e., it has the properties of the so-called cooperative paramagnet [5,92]. At the same time, the ground states formed directly at $\alpha = \pm 4$ are critical points, i.e., they also represent strongly correlated states of the model. All these facts allow one to consider the ground states formed at $\alpha = \pm 4$ as well as their close paramagnetic surroundings as regions with classical spin-liquid-like behavior present.

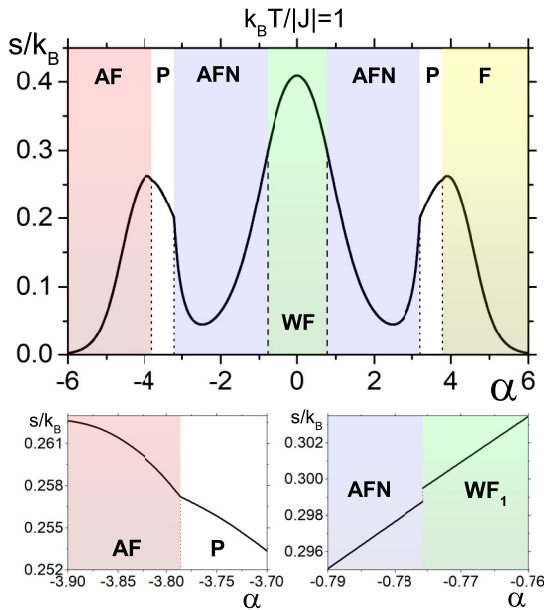


FIG. 23. Dependence of the entropy per site of the model on the parameter α for $k_B T/|J_1| = 1$ with two first-order (dashed vertical lines) and four second-order (dotted vertical lines) phase transitions explicitly present between corresponding phases.

V. CONCLUSION

Let us recapitulate the main results obtained in the present paper, where we have investigated the antiferromagnetic spin-1/2 Ising model on the three-dimensional octahedral lattice influenced by the presence of spin variables in the centers of all elementary octahedra with the ferromagnetic or the antiferromagnetic interactions between these central sites and the vertices of elementary octahedra. The properties of such a model on the BCO lattice were investigated using the recursive-lattice technique (approximation), in the framework of which the model was considered on the recursive BCO lattice that takes into account basic geometric properties of the regular BCO lattice responsible for frustration. The exact solution of the model was found, in the sense that the explicit expression for the free energy of the model as well as of the coordinates of the physically relevant stable fixed points of the corresponding system of recursion relations.

The phase diagram of the model was found and the positions of all phase transitions between various phases were determined. Moreover, the explicit form of the equation that drives the positions of all second-order phase transitions of the model was derived. It was shown that the general form

of the phase diagram is symmetric with respect to the sign of the interaction between the central sites and the vertex sites of elementary octahedra, i.e., it is the same regardless of the ferromagnetic or antiferromagnetic nature of this interaction. It was also shown that while the magnetization properties of the corresponding phases depend on whether the interaction is ferromagnetic or antiferromagnetic, their thermodynamic properties are completely the same.

One of the most interesting and important result of the present study is the fact that the so-called weak ferromagnetism, the existence of which in the antiferromagnetic systems on the octahedral lattice was predicted recently in the framework of the recursive-lattice approach [82] as well as in the framework of the corresponding effective field theory approximation [83], is preserved even in the studied classical spin-1/2 J_1 - J_2 model on the recursive BCO lattice regardless of the character (sign) of the interaction J_2 between the central sites and the vertex sites of the elementary octahedra. However, since the magnetization properties of the weak ferromagnetic phase for $J_2 < 0$ (the antiferromagnetic case) and $J_2 > 0$ (the ferromagnetic case) are different (see Figs. 4–7), two different weak ferromagnetic phases could be identified, which were denoted by WF_1 and WF_2 (see Fig. 10). From a physical point of view, this nontrivial conclusion can indicate that the phenomenon of weak ferromagnetism in antiferromagnetic systems on lattices with the octahedral structure is rather stable, in the sense that it can be observed even in rather large intervals of the parametric space of generalized models

(e.g., as in the studied model with spin variables in the centers of all elementary octahedra).

Our analysis also showed that another interesting phenomenon can exist under some conditions (at least in principle) in the magnetic systems on the BCO lattice. More specifically, it was shown that the paramagnetic phase can exist down to zero temperature in the studied magnetic system in the close vicinity of the highly macroscopically degenerated single-point-like ground states formed at $|\alpha| = |J_2/J_1| = 4$. Note that this high macroscopic degeneracy (the nonzero residual entropy) of these ground states is caused by the presence of frustration. Moreover, the paramagnetic phase in this region is bounded from the left and from the right by the curves of the second-order phase transitions (see Fig. 10) and therefore forms the so-called cooperative paramagnet [5]. All these facts, together with the fact that the ground states formed at $|\alpha| = 4$ are also critical points, allows one to consider the single-point-like ground states formed at $\alpha = \pm 4$ together with their immediate paramagnetic surroundings as potential regions with the existence of the classical spin-liquid-like behavior [5].

ACKNOWLEDGMENTS

This work was supported by the Slovak Research and Development Agency under Contract No. APVV-20-0293. This work was also supported by VEGA Grants No. 2/0044/23 and No. 2/0081/21 of the Slovak Academy of Sciences.

-
- [1] A. P. Ramirez, *Annu. Rev. Mater. Sci.* **24**, 453 (1994).
 - [2] J. E. Greedan, *J. Mater. Chem.* **11**, 37 (2001).
 - [3] R. Moessner, *Can. J. Phys.* **79**, 1283 (2001).
 - [4] J. Richter, J. Schulenburg, and A. Honecker, *Lect. Notes Phys.* **645**, 85 (2004).
 - [5] L. Balents, *Nature (London)* **464**, 199 (2010).
 - [6] J. S. Gardner, M. J. P. Gingras, and J. E. Greedan, *Rev. Mod. Phys.* **82**, 53 (2010).
 - [7] *Introduction to Frustrated Magnetism*, edited by C. Lacroix, P. Mendels, and F. Mila, Springer Series in Solid-State Sciences Vol. 164 (Springer, Berlin, 2011).
 - [8] *Frustrated Spin Systems*, edited by H. T. Diep (World Scientific, Singapore, 2013).
 - [9] L. Savary and L. Balents, *Rep. Prog. Phys.* **80**, 016502 (2017).
 - [10] *Frustrated Materials and Ferroic Glasses*, edited by T. Lookman and X. Ren (Springer Nature, Cham, 2018).
 - [11] G. Toulouse, *Commun. Phys.* **2**, 115 (1977).
 - [12] G. H. Wannier, *Phys. Rev.* **79**, 357 (1950).
 - [13] K. Kanô and S. Naya, *Prog. Theor. Phys.* **10**, 158 (1953).
 - [14] R. Liebmann, *Statistical Mechanics of Periodic Frustrated Ising Systems* (Springer, Berlin, 1986).
 - [15] A. P. Ramirez, A. Hayashi, R. J. Cava, R. Siddharthan, and B. S. Shastry, *Nature (London)* **399**, 333 (1999).
 - [16] K. Matsuhira, Z. Hiroi, T. Tayama, S. Takagi, and T. Sakakibara, *J. Phys.: Condens. Matter* **14**, L559 (2002).
 - [17] Z. Hiroi, K. Matsuhira, S. Takagi, T. Tayama, and T. Sakakibara, *J. Phys. Soc. Jpn.* **72**, 411 (2003).
 - [18] S. S. Sosin, L. A. Prozorova, A. I. Smirnov, A. I. Golov, I. B. Berkutov, O. A. Petrenko, G. Balakrishnan, and M. E. Zhitomirsky, *Phys. Rev. B* **71**, 094413 (2005).
 - [19] X. Ke, D. V. West, R. J. Cava, and P. Schiffer, *Phys. Rev. B* **80**, 144426 (2009).
 - [20] A. M. Hallas, A. M. Arevalo-Lopez, A. Z. Sharma, T. Munsie, J. P. Attfield, C. R. Wiebe, and G. M. Luke, *Phys. Rev. B* **91**, 104417 (2015).
 - [21] B. Wolf, U. Tutsch, S. Dörschung, C. Krellner, F. Ritter, W. Assmus, and M. Lang, *J. Appl. Phys.* **120**, 142112 (2016).
 - [22] E. Jurčišinová and M. Jurčišin, *Phys. Rev. E* **96**, 052128 (2017).
 - [23] S. Lucas, K. Grube, C.-L. Huang, A. Sakai, S. Wunderlich, E. L. Green, J. Wosnitzer, V. Fritsch, P. Gegenwart, O. Stockert, and H. v. Löhneysen, *Phys. Rev. Lett.* **118**, 107204 (2017).
 - [24] Y. Tokiwa, S. Bachus, K. Kavita, A. Jesche, A. A. Tsirlin, and P. Gegenwart, *Commun. Mater.* **2**, 42 (2020).
 - [25] M. Orendáč, P. Farkašovský, L. Regeciová, S. Gabáni, G. Pristáš, E. Gažo, J. Bačkai, P. Diko, A. Dukhnenko, N. Shitsevalova, K. Siemensmeyer, and K. Flachbart, *Phys. Rev. B* **102**, 174422 (2020).
 - [26] N. Terada and H. Mamyia, *Nat. Commun.* **12**, 1212 (2021).
 - [27] X. Tang, A. Sepehri-Amin, N. Terada, A. Martin-Cid, I. Kurniawan, S. Kobayashi, Y. Kotani, H. Takeya, J. Lai, Y. Matsushita, T. Ohkubo, Y. Miura, T. Nakamura, and K. Hono, *Nat. Commun.* **13**, 1817 (2022).
 - [28] E. Jurčišinová and M. Jurčišin, *J. Magn. Magn. Mater.* **572**, 170658 (2023).

- [29] Y. Zhou, K. Kanoda, and T.-K. Ng, *Rev. Mod. Phys.* **89**, 025003 (2017).
- [30] C. Broholm, R. J. Cava, S. A. Kivelson, D. G. Nocera, M. R. Norman, and T. Senthil, *Science* **367**, eaay0668 (2020).
- [31] V. Elser, *Phys. Rev. Lett.* **62**, 2405 (1989).
- [32] J. B. Marston and C. Zeng, *J. Appl. Phys.* **69**, 5962 (1991).
- [33] S. Sachdev, *Phys. Rev. B* **45**, 12377 (1992).
- [34] S. Yan, D. A. Huse, and S. R. White, *Science* **332**, 1173 (2011).
- [35] I. Rousochatzakis, R. Moessner, and J. van den Brink, *Phys. Rev. B* **88**, 195109 (2013).
- [36] R. Siddharthan and A. Georges, *Phys. Rev. B* **65**, 014417 (2001).
- [37] J. Richter, J. Schulenburg, P. Tomczak, and D. Schmalfuß, *Condens. Matter Phys.* **12**, 507 (2009).
- [38] H. Nakano and T. Sakai, *J. Phys. Soc. Jpn.* **82**, 083709 (2013).
- [39] A. Ralko and I. Rousochatzakis, *Phys. Rev. Lett.* **115**, 167202 (2015).
- [40] H. Nakano, Y. Hasegawa, and T. Sakai, *J. Phys. Soc. Jpn.* **84**, 114703 (2015).
- [41] K. Morita and T. Tohyama, *J. Phys. Soc. Jpn.* **87**, 043704 (2018).
- [42] T. Lugan, L. D. C. Jaubert, and A. Ralko, *Phys. Rev. Res.* **1**, 033147 (2019).
- [43] N. Astrakhantsev, F. Ferrari, N. Niggemann, T. Müller, A. Chauhan, A. Kshetrimayum, P. Ghosh, N. Regnault, R. Thomale, J. Reuther, T. Neupert, and Y. Iqbal, *Phys. Rev. B* **104**, L220408 (2021).
- [44] J. Richter, O. Derzhko, and J. Schnack, *Phys. Rev. B* **105**, 144427 (2022).
- [45] B. Liu, Z. Zeng, A. Xu, Y. Sun, O. Yakubovich, L. Shvanskaya, S. Li, and A. Vasiliev, *Phys. Rev. B* **105**, 155153 (2022).
- [46] P. Schmoll, A. Kshetrimayum, J. Naumann, J. Eisert, and Y. Iqbal, *Phys. Rev. B* **107**, 064406 (2023).
- [47] M. Gembé, H.-J. Schmidt, C. Hickey, J. Richter, Y. Iqbal, and S. Trebst, *Phys. Rev. Res.* **5**, 043204 (2023).
- [48] M. P. Shores, E. A. Nytko, B. M. Bartlett, and D. G. Nocera, *J. Am. Chem. Soc.* **127**, 13462 (2005).
- [49] T. H. Han, J. S. Helton, S. Chu, D. G. Nocera, J. A. Rodriguez-Rivera, C. Broholm, and Y. S. Lee, *Nature (London)* **492**, 406 (2012).
- [50] M. Fu, T. Imai, T.-H. Han, and Y. S. Lee, *Science* **350**, 655 (2015).
- [51] T. H. Han, M. R. Norman, J.-J. Wen, J. A. Rodriguez-Rivera, J. S. Helton, C. Broholm, and Y. S. Lee, *Phys. Rev. B* **94**, 060409(R) (2016).
- [52] Z. Feng, Z. Li, X. Meng, W. Yi, Y. Wei, J. Zhang, Y.-C. Wang, W. Jiang, Z. Liu, S. Li, F. Liu, J. Luo, S. Li, G.-q. Zheng, Z. Y. Meng, J.-W. Mei, and Y. Shi, *Chin. Phys. Lett.* **34**, 077502 (2017).
- [53] Y. Wei, Z. Feng, W. Lohstroh, D. H. Yu, D. Le, C. de la Cruz, W. Yi, Z. F. Ding, J. Zhang, C. Tan, L. Shu, Y.-C. Wang, H.-Q. Wu, J. Luo, J.-W. Mei, F. Yang, X.-L. Sheng, W. Li, Y. Qi, Z. Y. Meng, Y. Shi *et al.*, [arXiv:1710.02991](https://arxiv.org/abs/1710.02991).
- [54] Z. Feng, W. Yi, K. Zhu, Y. Wei, S. Miao, J. Ma, J. Luo, S. Li, Z. Y. Meng, and Y. Shi, *Chin. Phys. Lett.* **36**, 017502 (2018).
- [55] P. Khuntia, M. Velazquez, Q. Barthélemy, F. Bert, E. Kermarrec, A. Legros, B. Bernu, A. Z. L. Messio, and P. Mendels, *Nat. Phys.* **16**, 469 (2020).
- [56] Y. Wei, X. Ma, Z. Feng, Y. Zhang, L. Zhang, H. Yang, Y. Qi, Z. Y. Meng, Y.-C. Wang, Y. Shi, and S. Li, *Chin. Phys. Lett.* **38**, 097501 (2021).
- [57] Y. Fu, M.-L. Lin, L. Wang, Q. Liu, L. Huang, W. Jiang, Z. Hao, C. Liu, H. Zhang, X. Shi, J. Zhang, J. Dai, D. Yu, F. Ye, P. A. Lee, P.-H. Tan, and J.-W. Mei, *Nat. Commun.* **12**, 3048 (2021).
- [58] Z. Zeng, X. Ma, S. Wu, H.-F. Li, Z. Tao, X. Lu, X.-H. Chen, J.-X. Mi, S.-J. Song, G.-H. Cao, G. Che, K. Li, G. Li, H. Luo, Z. Y. Meng, and S. Li, *Phys. Rev. B* **105**, L121109 (2022).
- [59] M. Fujihala, K. Morita, R. Mole, S. Mitsuda, T. Tohyama, S.-I. Yano, D. Yu, S. Sota, T. Kuwai, A. Koda, H. Okabe, H. Lee, S. Itoh, T. Hawaii, T. Masuda, H. Sagayama, A. Matsuo, K. Kindo, S. Ohira-Kawamura, and K. Nakajima, *Nat. Commun.* **11**, 3429 (2020).
- [60] O. V. Yakubovich, L. V. Shvanskaya, G. V. Kiriukhina, A. S. Volkov, O. V. Dimitrova, and A. N. Vasiliev, *Inorg. Chem.* **60**, 11450 (2021).
- [61] M. M. Markina, P. S. Berdonosov, T. M. Vasilchikova, K. V. Zakharov, A. F. Murtaozov, V. A. Dolgikh, A. V. Moskvina, V. N. Glazkov, A. I. Smirnov, and A. N. Vasiliev, [arXiv:2212.11623](https://arxiv.org/abs/2212.11623).
- [62] N. Achiwa, T. Matsuyama, and T. Yoshinari, *Phase Transit.* **28**, 79 (1990).
- [63] G. Cao, J. Bolivar, S. McCall, J. E. Crow, and R. P. Guertin, *Phys. Rev. B* **57**, R11039 (1998).
- [64] X.-Y. Wang, L. Gan, S.-W. Zhang, and S. Gao, *Inorg. Chem.* **43**, 4615 (2004).
- [65] V. A. Khomchenko, D. A. Kiselev, J. M. Vieira, R. M. Rubinger, N. A. Sobolev, M. Kopcewicz, V. V. Shvartsman, P. Borisov, W. Kleemann, and A. L. Kholkin, *J. Phys.: Condens. Matter* **20**, 155207 (2008).
- [66] J.-H. Lee, Y. K. Jeong, J. H. Park, M.-A. Oak, H. M. Jang, J. Y. Son, and J. F. Scott, *Phys. Rev. Lett.* **107**, 117201 (2011).
- [67] D. Haskel, G. Fabbri, M. Zhernenkov, P. P. Kong, C. Q. Jin, G. Cao, and M. van Veenendaal, *Phys. Rev. Lett.* **109**, 027204 (2012).
- [68] G. Cao, A. Subedi, S. Calder, J.-Q. Yan, J. Yi, Z. Gai, L. Poudel, D. J. Singh, M. D. Lumsden, A. D. Christianson, B. C. Sales, and D. Mandrus, *Phys. Rev. B* **87**, 155136 (2013).
- [69] F. Ye, S. Chi, B. C. Chakoumakos, J. A. Fernandez-Baca, T. Qi, and G. Cao, *Phys. Rev. B* **87**, 140406(R) (2013).
- [70] S. Bahr, A. Alfonsov, G. Jackeli, G. Khaliullin, A. Matsumoto, T. Takayama, H. Takagi, B. Büchner, and V. Kataev, *Phys. Rev. B* **89**, 180401(R) (2014).
- [71] W.-Y. Lee, H. J. Yun, and J. W. Yoon, *J. Alloys Compd.* **583**, 320 (2014).
- [72] M. A. Ahmed, N. G. Imam, M. K. Abdelmaksoud, and Y. A. Saeid, *J. Rare Earths* **33**, 965 (2015).
- [73] W. K. Zhu, C.-K. Lu, W. Tong, J. M. Wang, H. D. Zhou, and S. X. Zhang, *Phys. Rev. B* **91**, 144408 (2015).
- [74] Y. Cao, M. Xiang, W. Zhao, G. Wang, Z. Feng, B. Kang, A. Stroppa, J. Zhang, W. Ren, and S. Cao, *J. Appl. Phys.* **119**, 063904 (2016).
- [75] V. Fuster, M. C. Blancob, D. G. Francoc, G. Tiraod, V. M. Nassife, G. Nievac, and R. E. Carbonio, *J. Alloys Compd.* **681**, 444 (2016).

- [76] J. Zang, G. Zhou, Y. Bai, Z. Quan, and X. Xu, *Sci. Rep.* **7**, 10557 (2017).
- [77] F. Pomiro, D. M. Gil, V. Nassif, A. Paesano, M. I. Gomez, J. Guimpel, R. D. Sanchez, and R. E. Carbonio, *Mater. Res. Bull.* **94**, 472 (2017).
- [78] G. Park, I.-H. Oh, J. M. Sungil Park, S.-H. Park, C. S. Hong, and K.-S. Lee, *Phys. B: Condens. Matter* **551**, 89 (2018).
- [79] M. Jeddi, H. Gharsallah, M. Bejar, M. Bekri, E. Dhahri, and E. K. Hlil, *RSC Adv.* **8**, 9430 (2018).
- [80] Q. Liu, X.-X. Wang, C. Song, J.-X. Sui, X. Yan, J.-C. Zhang, H.-S. Zhao, F. Yuan, and Y.-Z. Long, *J. Magn. Magn. Mater.* **469**, 76 (2019).
- [81] J.-S. Zhou, L. G. Marshall, Z.-Y. Li, X. Li, and J.-M. He, *Phys. Rev. B* **102**, 104420 (2020).
- [82] E. Jurčišinová and M. Jurčičin, *J. Magn. Magn. Mater.* **513**, 167085 (2020).
- [83] E. Jurčišinová and M. Jurčičin, *Europhys. Lett.* **132**, 37004 (2020).
- [84] R. J. Baxter, *Exactly Solved Models in Statistical Mechanics* (Academic, London, 1982).
- [85] P. D. Gujrati, *Phys. Rev. Lett.* **74**, 809 (1995).
- [86] W. F. Wolff and J. Zittartz, *J. Magn. Magn. Mater.* **54–57**, 144 (1986).
- [87] W. R. Chen, F. C. Zhang, J. Miao, B. Xu, X. L. Dong, L. X. Cao, X. G. Qiu, B. R. Zhao, and P. Dai, *Appl. Phys. Lett.* **87**, 042508 (2005).
- [88] N. R. Kumar, R. Karthik, L. Vasylechko, and R. K. Selvan, *J. Phys.: Condens. Matter* **32**, 245802 (2020).
- [89] N. Martin, L. J. Bannenberg, M. Deutsch, C. Pappas, G. Chaboussant, R. Cubitt, and I. Mirebeau, *Sci. Rep.* **11**, 20753 (2021).
- [90] E. Jurčišinová and M. Jurčičin, *J. Magn. Magn. Mater.* **524**, 167658 (2021).
- [91] S. V. Isakov, K. S. Raman, R. Moessner, and S. L. Sondhi, *Phys. Rev. B* **70**, 104418 (2004).
- [92] J. Villain, *Z. Phys. B* **33**, 31 (1979).